Econ. Environ. Geol.
Vol. 28, No. 4, p. 337-350, 1995.

Geochemistry and Genesis of Hydrothermal Cu Deposits in the Gyeongsang Basin, Korea : Hwacheon-ri Mineralized Area

Chil-Sup So*, Sang-Hoon Choi** and Seong-Taek Yun***

ABSTRACT : The Hwacheon-ri mineralized area is located within the Cretaceous Gyeongsang Basin of the Korean peninsula. The mineralized area includes the Hwacheon, Daeweon, Kuryong and Cheongryong mines. Each of these mines occurs along copper-bearing hydrothermal quartz veins that crosscut late Cretaceous volcanic rocks, although some disseminated ores in host rocks also exist locally. Mineralization can be separated into three distinct stages (I, II, and III) which developed along preexisting fracture zones. Stage I is ore-bearing, whereas stages II and III are barren. The main phase of ore mineralization, stage I, can be classified into three substages (Ia, Ib and Ic) based on ore mineral assemblages and textures. Substage Ia is characterized by pyrite-arsenopyrite-molybdenite-pyrrhotite assemblage and is most common at the Hwacheon deposit. Substage Ib is represented by main precipitation of Cu, Zn, and Pb minerals. Substage Ic is characteristic of hematite occurrence and is shown only at the Kuryong and Cheongryong deposits. Some differences in the ore mineralization at each mine in the area suggest that the evolution of hydrothermal fluids in the area varied in space (both vertically and horizontally) with respect to igneous rocks relating the ore mineralization. Fluid inclusion data show that stage I ore mineralization mainly occurred at temperatures between $\approx 350^{\circ}$ and $\approx 200^{\circ}C$ from fluids with salinities between 9.2 and 0.5 wt.% eq. NaCl. In the waning period of substage Ia, the high temperature and salinity fluid gave way to progressively cooler, more dilute fluids of later substage Ib and Ic (down to 200℃, 0 wt.% NaCl). There is a systematic decrease in the calculated $\delta^{18}O_{H2O}$ values with paragenetic time in the Hwacheon-ri hydrothermal system from values of $\approx 2.7‰$ for substage Ia, through $\approx -2.8‰$ for substage Ib, to $\approx -9.9‰$ for substage Ic. The δD values of fluid inclusion water also decrease with decreasing temperature (except for the Daeweon deposit) from −62‰ (substage Ia) to −80‰ (substage Ic and stage III). These trends are interpreted to indicate the progressive cooler, more oxidizing unexchanged meteoric water inundation of an initial hydrothermal system which is composed of highly exchanged meteoric water. Equilibrium thermodynamic interpretation of the mineral assemblages with the variation in amounts of chalcopyrite through the paragenetic time, and the evolution of the Hwacheon-ri hydrothermal fluids indicate that the solubility of copper chloride complexes in the hydrothermal system was mainly controlled by the variation of temperature and fo_2 conditions.

INTRODUCTION

The Gyeongsang Basin lies on the southeastern margin of the Korean peninsula and is filled by a mixed sequence of Cretaceous sedimentary and volcanic rocks intruded by igneous rocks of the Cretaceous to Tertiary (Fig. 1). Enclosed within the volcanic and sedimentary (rarely igneous) rocks of Cretaceous age are a number of fissure-filling hydrothermal veins (and/or disseminated ore deposits) containing mostly copper, zinc, lead, and/or tungsten and molybdenum minerals. The deposits display differences in mineralogy, paragenesis, mineralization temperature, fluid compositions, isotopic signature, and evolution of the hydrothermal fluids (Park *et al.*, 1983 and 1985; So *et al.*, 1985; Choi and So, 1992; Choi *et al.*, 1993 and 1994). Some of the copper and molybdenum mineralizations in the basin show noncommercial porphyry type affinities (Sillitoe, 1980). These may indicate that the evolution of hydrothermal fluids in the basin varied in time and space of mineralization with respect to granitic magmatism.

The Hwacheon-ri area contains a number of fissure-filling, polymetallic hydrothermal quartz veins (including locally disseminated ores). The Hwacheon, Daeweon, Kuryong, and Cheongryong mines are located on such veins. Sillitoe (1980) discussed that the Hwacheon and Kuryong mine areas are one of the porphyry type mineralization areas in the basin based on the hydro-

*Dept. of Earth and Environmental Sciences, Korea Univ., Seoul 136-701, Korea
**Center for Mineral Resources Research, Korea Univ., Seoul 136-701, Korea
***Department of Mineral and Energy Resources Engineering, Semyung University, Jecheon 390-230, Korea

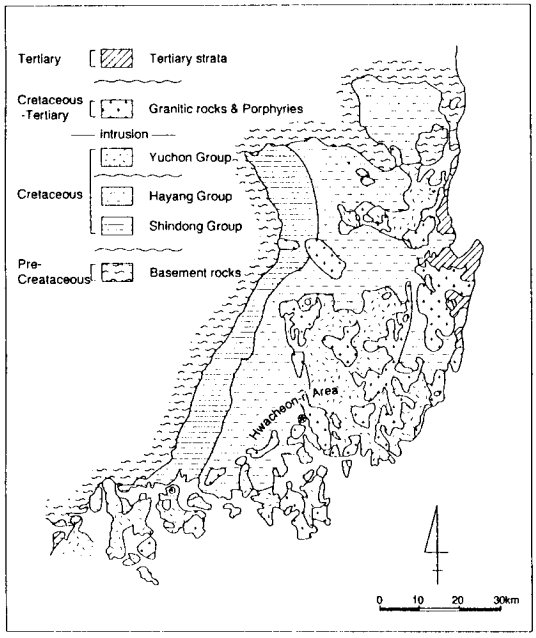

Fig. 1. Simplified geologic map of the Gyeongsang Basin, Korea, showing the location of the Hwacheon-ri mineralized area.

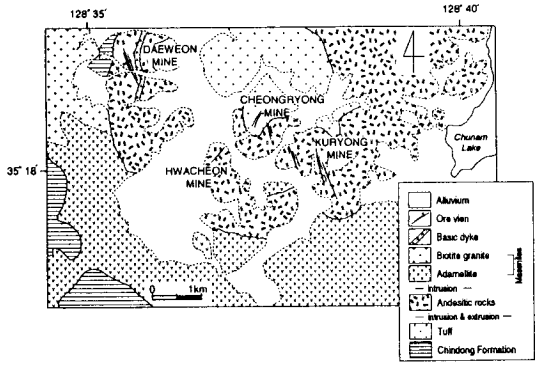

Fig. 2. Local geologic map of the Hwacheon-ri mineralized area.

thermally altered zone and mineralization at Kuryong. We know of no previous studies concerning the physical and chemical conditions of ore deposition of the deposits in the Hwacheon-ri area. This paper presents the results of our investigation of the nature of the mineralization in the Hwacheon-ri mineralized area.

GEOLOGY

The Hwacheon-ri area is located approximately 400 km southeast of Seoul along the southern margin of the Gyeongsang Basin. Rocks in the mineralized area consist of the sedimentary Chindong Formation, volcanic rocks, and younger calc-alkaline igneous rocks (Fig. 2). The Hwacheon, Kuryong, Cheongryong, and Daeweon deposits are enclosed within the andesitic volcanic rocks.

The sedimentary Chindong Formation is uppermost of the units of Middle Cretaceous Hayang Group, and crops out in the southwestern part of the area. The Chindong Formation, ≤1,500 m thick (Lee, 1987), strikes N25° to 40°E, dips 5° to 15°SE and is composed mainly of grey shale interlayered with minor sandstone. The Palyongsan tuff is compositionally dacitic tuff within which thin beds of grey sandstone are locally interbedded, and distributes in the northern part of the area.

Upper Cretaceous volcanic rocks are predominantly andesitic rocks (Chusan andesitic rock; Kim and Kim, 1963). The andesitic rocks commonly intruded or conformably cover the early sedimentary rocks (mainly Chindong Formation) around the area. The Chusan andesitic rocks is composed of andesite, augite andesite, hornblende andesite, trachy andesite, and brecciated andesite (Kim and Kim, 1963). Trachy andesite (with propylite) is the most common in the Hwacheon-ri area. They generally contain plagioclase phenocrysts in a matrix of lath-shaped plagioclase crystals and fine-grained quartz, together with small amounts of iron oxides, augite, and glass. It is strongly altered locally at Hwacheon and Kuryong mine area.

Late Cretaceous granitic rocks occur as small stocks in the area and are mainly composed of adamellite and biotite granite, called the masanites (the Masan granites). These granitic rocks, the youngest members of the Bulgugsa Series, are restricted to the southeastern portion of the Gyeongsang Basin. The rocks are highly differentiated and display a compositional trend from tonalite through adamellite and micrographic granite to granite porphyry, which are considered to be evolved Bulgugsa magmas (Iiyama and Fonteilles, 1981; Ishihara *et al.*, 1981; Jin *et al.*, 1981). Adamellite shows locally a conspicuous micrographic texture (graphic adamellite) in which quartz and orthoclase are intergrown vermicularly. It shows increasing tendency of biotite and orthoclase and grades into biotite granite in the western portion of Daeweon mine area (at northeastern edge in the area; Fig. 2).

ORE VEINS

Within the Hwacheon-ri area, a number of hydrothermal metal-bearing quartz veins, and barren quartz (or chalcedony) and calcite veins with locally irregular

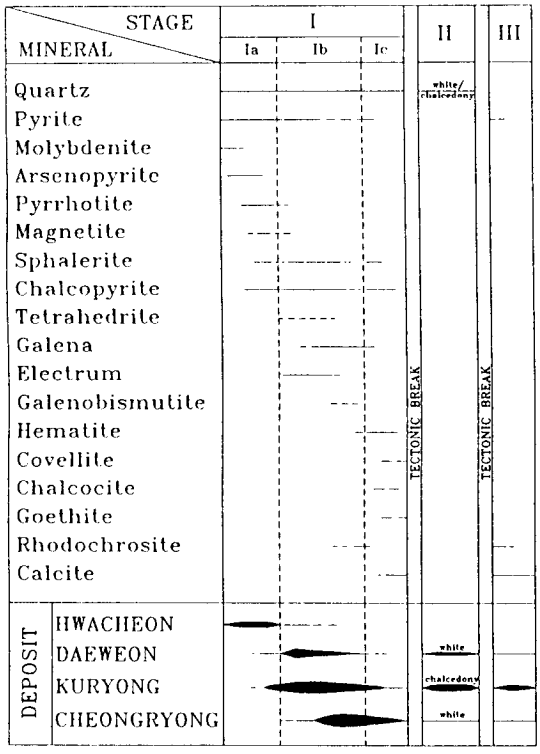

Fig. 3. Generalized paragenetic sequence of minerals from the Hwacheon-ri mineralized area.

disseminated ores (mainly occur at Hwacheon and Kuryong mine area) were formed by filling of narrow open-space fractures in Cretaceous volcanic rocks. The veins can be divided into two sets according to their strikes: 1) the first set strikes N30°W to NS (main veins at the Kuryong and Daeweon mines with small veins at other mines); 2) the second strikes N20°W to N45°W (mainly at the Cheongryong mine). The veins of the second set are relatively small in size. The veins show textural evidence of open-space filling (internal mineral zonation), extend ≈ 300 m along strike, and vary in width from ≤20 to 100 cm. At the Daeweon and Kuryong mines, the ore veins generally display repeated pinching and swelling along strike and dip direction with concomitant lens-shaped ore shoot.

The veins are mineralogically polymetallic, consisting mainly of grey to white quartz with base-metal sulfides and carbonates. The veins and disseminated ores of Hwacheon mine have a relatively higher concentration of pyrite, arsenopyrite, pyrrhotite and molybdenite (early minerals of substage Ia; see "Mineralogy and Paragenesis" and Fig. 3) with lesser amounts of (or not found) chalcopyrite, sphalerite, and galena than the veins of the other three mines in the area. In the Kuryong mine, the main ore veins display lateral asymmetrical zoning of sulfide minerals with quartz and calcite, from vein margins to centers: pyrite(-arsenopyrite), massive chalcopyrite, chalcopyrite-sphalerite-galena with grey quartz, and calcite barren clear quartz. The veins are often cut or reopended and filled by chalcedony and calcite veining. In the Daeweon and Cheongryong mines, quartz veins contain lager concentration of sphalerite and galena than the Hwacheon and Kuryong mines. On the other hand, the veins in the Kuryong and Cheongryong mines are characterized by hematite occurrence and chalcopyrite (±pyrite) precipitation in vugs in quartz as the late vein mineralization of the mines. Some differences in the mineralization (such as mineralogy, paragenesis and amounts of each sulfide; Fig. 3) at each mine in the area may indicate that the evolution of hydrothermal fluids in the area varied in space (vertically and horizontally) with respect to igneous rocks relating the ore mineralization.

MINERALOGY AND PARAGENESIS

Three distinct stages have been determined on the basis of textural relationships (Fig. 3). Stage I volumetrically dominates mineralization with mainly grey to white quartz, sulfides, minor Fe-oxides, sulfosalts, and carbonates. Stage II mineralization is characterized by chalcedony (Kuryong deposits) or white to clear quartz (Daeweon and Cheongryong deposits) and minor sulfides. Stage III is a massive carbonate stage containing no ore mineral.

Stage I

Stage I is the dominant ore stage in the deposits from both a volumetric and economic standpoints. Veins penetrate pre-existing fractures and highly brecciated wallrock. Based on the textural relationships and mineral assemblages, it can be divided into three substages (Ia, Ib, and Ic; Fig. 3). Substage Ia is characterized by pyrite-arsenopyrite-pyrrhotite-chalcopyrite assemblage and is the most common at the Hwacheon deposit. Substage Ib is represented by main precipitation of Cu, Zn, and Pb minerals with rare electrum. Hematite occurrence is characteristic of substage Ic. This substage mineralization is shown only at the Kuryong and Cheongryong deposits (Fig. 3).

Substage Ia: Pyrite within fine-grained grey quartz and local molybdenite occurrence characterize early mineralization in the deposits. The main ore minerals are pyrite, molybdenite, arsenopyrite, and chalcopyrite

with minor pyrrhotite, magnetite, and sphalerite.

Pyrite, the dominant ore mineral in the deposits, occurs as subhedral to euhedral massive aggregates and are sometimes intergrown with arsenopyrite (30.3~31.5 atomic % As). It includes small grains of pyrrhotite, magnetite, and sphalerite. Molybdenite occurs as disseminations in the vein margins or around of wall rock fragments in the vein. Chalcopyrite is the dominant sulfide mineral at later period in substage Ia, and it is present both as anhedral masses with pyrite (± sphalerite) and disseminated, anhedral grains throughout the quartz. Small round-shaped inclusions of chalcopyrite are shown within pyrite. Early, dark brown sphalerite is enclosed within pyrite. Electron probe microanalysis of the sphalerite reveals higher FeS compositional ranges, than those of later sphalerites, from 10.2 to 11.0 mole percent FeS.

Substage Ib: Economic quantities of Cu-Zn-Pb minerals with rare electrum were introduced during substage Ib together with other sulfides and sulfosalts. Minerals of this substage are characterized by variable proportions of chalcopyrite, sphalerite, galena, and pyrite with minor amounts of tetrahedrite, electrum, and galenobismutite.

Chalcopyrite occurs as irregular masses and veinlets, and coarse-grained disseminations in substage Ib. It is commonly associated with pyrite + sphalerite (early period of substage Ib) and sphalerite + galena (later period of substage Ib) that cut pyrite along fractures. Sometimes, it includes sphalerite and euhedral to subhedral pyrite. Sphalerite is distributed widely throughout the paragenesis of substage Ib mineralization and occurs as: 1) partly intergrowths with pyrite and as anhedral masses cut by chalcopyrite (this form has relatively high FeS contents (3.0~4.6 mole % FeS)); 2) polycrystalline aggregates associated with galena and tiny veinlets that generally cut chalcopyrite. The later sphalerite, which has 1.7 to 2.7 mole percent FeS, is cemented and replaced by galena and galenobismutite. Tetrahedrite is generally associated with early galena and is found penetrating chalcopyrite and sphalerite along fractures. Electrum (N_{Ag}=0.41~0.55) occurs as rounded or irregular inclusions in sphalerite and galena.

Substage Ic: Hematite is introduced during substage Ic mineralization. The main ore minerals are sphalerite, chalcopyrite, pyrite, and hematite with lesser amounts of covellite, chalcocite, and goethite as replacement products. Gangue minerals are principally grey to white quartz with rare clear euhedral quartz and calcite. Clear quartz rhythmically overgrows earlier white quartz at or near vugs. Honney yellow sphalerite occurs as commonly polycrystalline aggregates associated with late galena and/or is shown at or near vugs. The sphalerite has the lowest FeS contents (≤0.94 mole % FeS) among sphalerites from the deposits. Subhedral to euhedral chalcopyrite and/or pyrite generally occur in vugs in quartz as the latest ore mineralization in stage I veins. Hematite occurs as euhedral specularite crystals, and is commonly interstitial to euhedral quartz crystals or in fractures of pyrite. Hematite is characteristic of all later stage I mineralization, especially, in the Kuryong and Cheongryong deposits. The hematite occurrence combined with compositional variations of the sphalerite, and chalcopyrite and pyrite occurrences in vugs as the latest ore mineralization suggest a distinct change in fluid conditions at later period in stage I.

Stage II

Stage II is characterized by white quartz (Daeweon and Cheongryong deposits) or a dark-grey, waxy chalcedony (Kuryong deposit). Locally, veins contain highly silicified, brecciated fragments of wallrock. Pyrite and chalcopyrite constitute a small proportion of the veins and are found as disseminations only within white quartz. The chalcedony vein of stage II has been locally cut and obliterated by younger stage III calcite vein. The stage II chalcedony occurs dominantly at Kuryong deposit.

Stage III

Stage III is characterized by narrow (≈0.2~10 cm) veins or veinlets of white to clear calcite with variable attitudes that occur in or near veins of earlier stages. The veins commonly do not contain ore minerals, although small amounts of pyrite occur locally in the stage III calcite vein at Kuryong. The veins are best displayed in the Kuryong deposit.

FLUID INCLUSION STUDIES

Fluid inclusions were examined in more than 90 samples of grey to white and clear quartz, sphalerite, and calcite of hydrothermal veins from deposits in the Hwacheon-ri area. Fluid inclusions were examined in thin (1mm or less) doubly polished plates. Microthermometric measurements were made on a Fluid Inc. gas-flow heating-freezing system. Replicate measurements of homogenization temperatures showed a reproducibility within ±2.0℃ at temperatures near 350℃. Replicate measurements of melting temperatures of H_2O-rich standard fluid inclusions showed a reproducibility within ±0.2℃. The salinity data reported are based on

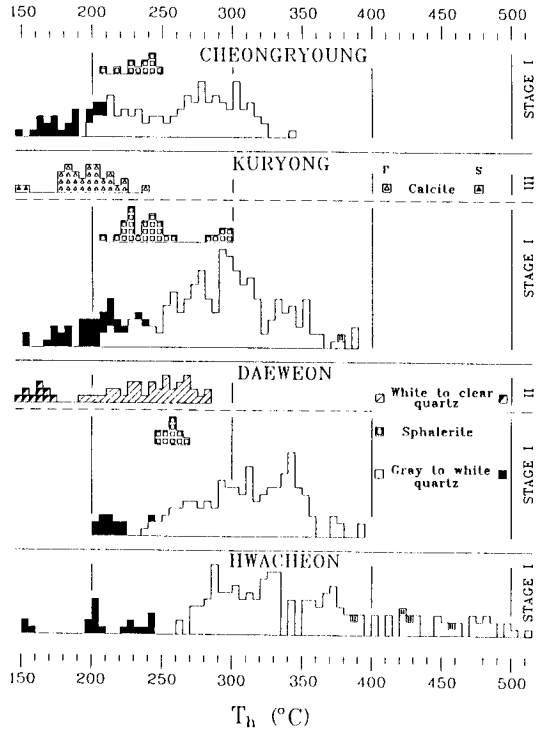

Fig. 4. Histograms of total homogenization temperatures of fluid inclusions in vein minerals from each mine in the Hwacheon-ri mineralized area.

freezing point depression in the system H_2O-NaCl (Potter *et al.*, 1978). The results of the heating and freezing experiments are presented in Fig.s 4 through 6.

Types of Fluid Inclusions

Only two types of primary and secondary fluid inclusions were observed: types I (liquid-rich) and II(vapour-rich).

Type I : Liquid-rich, two-phase fluid inclusions are the predominant type in the area and contain a liquid and a vapor bubbles that form generally 10~20 volume percent of the fluid inclusion at room temperature. This type of fluid inclusions occurs as primary and secondary inclusions, with variable size from ≤5 to 80 μnm (generally 15~25 μm). The primary fluid inclusions, which show commonly uniform size (≈ 20 μm), are generally simple and subrounded, tabular or negative crystal forms in shape. These fluid inclusions contain no daughter minerals and homogenize readily to the liquid phase.

Type II : Vapor-rich, two-phase fluid inclusions contain a liquid and a vapor bubbles that occupy about 70 to 80 volume percent of the fluid inclusion at room temperature. These homogenize to the vapor phase and occur only as primary fluid inclusions in grey quartz from early stage I veins of the Hwacheon and Kuryong deposits. No traces of gas hydrates were observed during freezing, indicating that CO_2 concentrations are below that required to form clathrates (≤0.85 molal; Hedenquist and Henley, 1985).

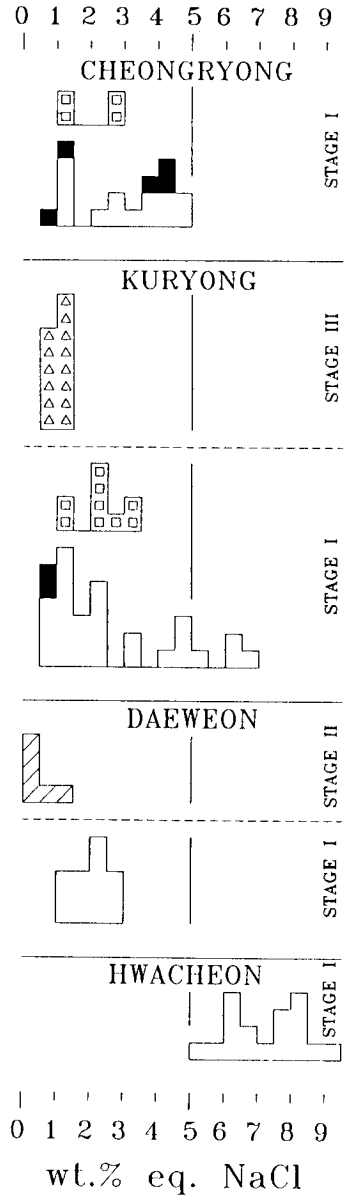

Fig. 5. Histograms of salinities of fluid inclusions in vein minerals from each mine in the Hwacheon-ri mineralized area. Symbols are the same as in Fig. 4.

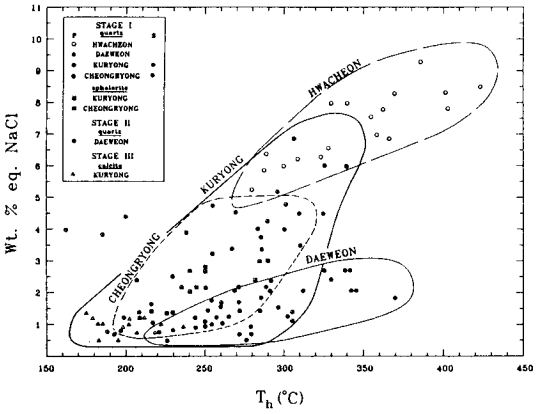

Fig. 6. Total homogenization temperature versus salinity diagram for fluid inclusions in stage I minerals from each mine in the Hwacheon-ri mineralized area.

The wide range of homogenization temperatures of primary fluid inclusions in quartz samples from stage I veins may reflect a continuum of several hydrothermal episodes rather than one specific event. However, by analyzing peaks within frequency diagrams of fluid inclusion data (Figs. 4, 5, and 6), it may be possible to decipher individual hydrothermal events which may be related to specific mineral assemblages.

Fluid Inclusions in Stage I Veins

Minerals examined were grey to white quartz and sphalerite. Primary type I fluid inclusions in stage I grey to white quartz homogenize from 198℃ to 511℃ (Hwacheon deposit, 261°~511°; Daeweon deposit, 237°~394℃; Kuryong deposit, 207°~383℃; Cheongryong deposit, 198°~343℃). Vapor-rich type II fluid inclusions in stage I quartz were found only in the Hwacheon and Kuryong deposits. Limited data were obtained from the type II fluid inclusions owing to the small size for heating and freezing experiments. They homogenize from 371° to 455℃ (Hwacheon deposit, 385°~455℃; Kuryong deposit, 371℃). Primary type I fluid inclusion in main to late (substage Ib to Ic) sphalerite homogenize at temperatures between 208° and 299℃ (Fig. 4).

Only a few type I fluid inclusions were large enough for freezing experiments. The salinities of these fluids in stage I quartz and sphalerite from the deposits range from 0.5 to 9.2 (Hwacheon deposit, 5.3~9.2; Daeweon deposit, 1.0~2.7; Kuryong deposit, 0.5~6.9; Cheongryong deposit, 1.1~4.8) and 1.2 to 3.0 (Kuryong deposit, 1.4~3.0; Cheongryong deposit, 1.2~2.8) wt. percent eq. NaCl, respectively (Fig. 5).

Fluid Inclusions in Stage II and III veins

Only type I fluid inclusions were found in stage II white quartz and stage III calcite. Primary type I fluid inclusions in stage II white quartz from the Daeweon deposit homogenize at temperatures of 192° to 283℃ (Fig. 4), and have salinities between 0.5 and 1.7 wt. percent eq., NaCl (Fig. 5).

Stage III calcite contains primary fluid inclusions which homogenize at temperatures between 175° and 236℃, with salinities between 0.5 and 1.4 wt. percent eq. NaCl (Figs. 4 and 5).

Variations in Temperature and Composition of Hydrothermal Fluids

Variations in temperature and composition of the hydrothermal fluids during mineralization episodes are recorded by fluid inclusions. The homogenization temperatures of primary fluid inclusions in minerals of stage I range from 198° to 511℃ and salinities are between 0.5 and 9.2 wt. percent eq. NaCl. Over this wide range of temperatures and salinities an analysis of clusters of data in each deposit has made it possible to distinguish individual events that are probably related to a specific mineral paragenesis. The relationship between homogenization temperatures and salinities of fluid inclusions in stage I, II, and III vein minerals from the deposits in the area (Fig. 6) indicates a fluid evolution history of cooling and dilution by mixing after boiling (see below).

Most of the vapor-rich type II fluid inclusions are found limited to samples only in Hwacheon and Kuryong deposits and are very small for fluid inclusion study (especially, for freezing experiment), but some fluid inclusions homogenize at temperatures in the range of 371°~455℃ (Fig. 4). These fluid inclusions were trapped simultaneously with type I fluid inclusions under the same temperature range, a conclusion that was supported by microscopic observation. Therefore, during early mineralization in the area the boiling of ore fluids resulted in an increase in fluid salinity (up to 9.2 equiv. wt. % NaCl) at temperatures near ≥380℃. Later cooling and dilution of the hydrothermal fluids by mixing with cooler, less saline and less evolved meteoric waters resulted in the positive linear relationship between temperature and salinity that is apparent in Fig. 6. Fluids evolved from a high-temperature, high-salinity end-member towards a low-temperature, less saline component (down to 200℃ and 0.5 equiv. wt. % NaCl). By the advent of stage II white to clear quartz and stage III calcite deposition cooling and dilution were more pronounced

Table 1. Sulfur isotope data of stage I sulfide minerals from the Hwacheon-ri area.

Mine	Sample	Substage	Mineral	$\delta^{34}S(‰)$	$\Delta^{34}S(‰)$	T(℃)[1]	T(℃)[2]	$\delta^{34}S_{H2S}(‰)$[3]
Hwacheon	HC-3	Ia	Pyrite	3.7			340	2.6
Daeweon	TW-50-1	Ib	Chalcopyrite	4.9			310	5.0
	TW-50-2	Ic	Galena	−0.1			240	2.2
	TW-50-3	Ib	Sphalerite	3.3			260	3.0
Kuryong	KR-27	Ic	Galena	−0.7			230	1.8
	KR-31-1	Ib	Chalcopyrite	3.1			280	3.3
	KR-31-2	Ib	Sphalerite	2.9	2.7	244 ± 35	244	2.5
	KR-31-3	Ib	Galena	0.2			244	2.5
	KR-38-1	Ib	Chalcopyrite	3.6			300	3.7
	KR-38-2	Ia	Pyrite	3.4			340	2.3
Cheongryong	CR-5-3	Ib	Sphalerite	4.4			260	4.1
	CR-5-4	Ic	Galena	−0.9			230	1.6

[1] Calculated sulfur isotope temperatures using compiled data of Ohmoto and Rye (1979)
[2] Based on fluid inclusion and/or sulfur isotope temperatures
[3] Calculated using the sulfur isotope fractionation equations in Ohmoto and Rye (1979).

Table 2. Carbon, Oxygen, and hydrogen isotope data for various minerals and inclusions fluids from the Hwacheon-ri area.

Mine	Sample no.	Stage	Mineral	$\delta^{13}C(‰)$	$\delta^{18}O(‰)$	T(℃)[1]	$\delta^{18}O_{water}(‰)$	$\delta D_{water}(‰)$	Remark
Hwacheon	HC-4	Ia	quartz		7.5	370	2.7	−65	Associated with py+po+asp
Daeweon	TW-14	Ia	quartz		6.8	330	0.9	−79	Associated with sp+cp
	TW-50	Ib	quartz		5.2	300	−1.7	−80	Associated with sp+gn
Kuryong	KR-2	Ia	quartz		8.1	320	1.9	−62	Associated with py
	KR-31	Ib	quartz		4.4	290	−2.8	−71	Associated with massive cp
	KR-49	III	calcite	−7.1	3.4	195	−6.4	−76	
	KR-65	III	calcite	−7.5	3.9	195	−5.9	−75	
Cheongryong	CR-1	Ic	quartz		−0.3	235	−9.9	−79	Clear crystals near vugs
	CR-22	Ib	quartz		2.4	270	−5.6	−72	Associated with sp+gn

[1] Based on fluid inclusion temperatures and paragenetic constraints
[2] Calculated using the quartz-water oxygen isotope fractionation equation of Matsuhisa *et al.* (1979)
Abbreviations : asp=arsenopyrite, cp=chalcopyrite, gn=galena, po=pyrrhotite, py=pyrite, sp=sphalerite.

(temperature, to 175℃; salinity, 0.5 equiv. wt. % NaCl), probably owing to repeated fracturing that allowed more dilute meteoric water into the system.

The deposits in the area generally display similarities in mineralogy and fluid evolution histories (temperature-salinity relationships, Fig. 6). In detail, however, the paragenetic mineral assemblages (Fig. 3), fluid compositions, and homogenization temperatures in each deposit are different. Early (substage Ia) mineral paragenesis is the most common at the Hwacheon deposit. Additionally, the Hwacheon deposit display relatively high homogenization temperature and salinity cluster. Whereas, the Kuryong and Cheongryong deposits are characterized by dominant substage Ib and Ic mineralization and showed relatively lower homogenization temperature and salinity cluster. Especially, the Daeweon deposit is represented by lower salinities than those of the same temperature range of the other deposits (Figs. 5 and 6). This may indicate that the initial hydrothermal fluids at Daeweon are relatively moderately evolved meteoric water reflecting moderate ratios of water to rock (see section on Stable Isotope Studies). In summary, fluid evolution history of the fluids at each deposit in the area generally indicates cooling and dilution by mixing after boiling, but the dominant mineral paragenesis and the range of temperatures and salinities are different. These may indicate that the evolution of hydrothermal fluids in the studied area varied in space and time with respect to wall rocks and granitic magmatism.

Pressure Consideration

Type I and II fluid inclusions are intimately associated in some samples of early stage I quartz from the Hwacheon and Kuryong deposits and homogenize at the same temperature range from 371° to 455℃. These observations indicate that fluids which deposited vein minerals during early mineralization of stage I boiled. Data for the system H_2O-NaCl (Haas, 1971; Cunningham, 1978) combined with the temperature and salinity data for these fluid inclusions, indicate pressures of about

≤300 to 470 bars. These may be maximum pressure of the deposits (especially, the Hwacheon and Kuryong deposits) in the area. These pressures correspond to maximum depths of about 1000 to 1800 m, assuming lithostatic loads.

STABLE ISOTOPE STUDIES

Recent studies have demonstrated the usefulness of stable isotopes in elucidating the origin and history of hydrothermal fluids and their constituents in vein-type deposits. In this study we measured the C, O, H, and S isotope compositions of quartz, calcite, sulfides, and fluid inclusion waters. Standard techniques for extraction and analysis were used (McCrea, 1950; Grinenko, 1962; Roedder *et al.*, 1963; Hall and Friedman, 1963; Rye, 1966). Isotope data are reported in standard e notation relative to the PDB standard for C, SMOW for O and H, and CDT for S. The analytical error is approximately ±0.1 per mil for C, O and S; ±2 per mil for H (Tables 1 and 2).

Sulfur Isotope Study

The $\delta^{34}S$ values (per mil) of eleven hand-picked sulfides from veins of each deposit in the area have the following values (Table 1): pyrite (3.4 and 3.7); chalcopyrite (3.1 to 4.9); sphalerite (2.9 to 4.4); galena (−0.9 to 0.2). Sulfur isotope compositions in stage I sulfides of the deposits have a narrow range of values betwen −0.9 and 4.9 per mil. One sphalerite-galena pair from substage Ib vein of the Kuryong deposit with texture suggesting coprecipitation of the phases has $\Delta^{34}S$ value 2.7 per mil. Using the sphalerite-galena sulfur isotope fractionation equation of Ohmoto and Rye (1979), the apparent equilibrium isotope temperature of the phases is 244±35℃.

Using temperatures estimated from fluid inclusions, paragenetic constraints, and sulfur isotope pair, the calculated $\delta^{34}S$ values of H_2S in stage I hydrothermal fluids are 1.4 to 5.0 per mil (pyrite, 2.3 and 2.6‰; chalcopyrite, 3.3 to 5.0‰; sphalerite, 2.5 to 4.0‰; galena, 1.4 to 2.5‰; Table 1) (Ohmoto and Rye, 1979). The overlap of the ranges suggests that a fluid with a mean $\delta^{34}S_{H_2S}$ value of about 3.0 per mil was responsible for the mineralization in the studied area. Ore and alteration mineral assemblages indicate that sulfur in the hydrothermal fluids was dominantly H_2S.

Therefore, the $\delta^{34}S$ values of H_2S are a good approximation of the $\delta^{34}S_{\Sigma S}$ values of the fluid. We interpret these values to represent an igneous source of sulfur, likely the nearby Cretaceous igneous rocks (Masanites and/or volcanic rocks; see Fig. 2).

Oxygen and Hydrogen Isotope Studies

The $\delta^{18}O$ values of seven quartz samples from stage I (each substage) of the deposits in the area range from −0.3 to 8.1 per mil (Hwacheon, 7.5‰; Daeweon, 5.2 and 6.8‰; Kuryong, 4.4 and 8.1‰; Cheongryong, −0.3 and 2.4‰) (Table 2). Using the quartz-water oxygen isotope fractionation equation of Matsuhisa *et al.* (1979), coupled with fluid inclusion temperatures of each sample, the calculated oxygen isotope compositions of waters in equilibrium with the stage I quartz range from −9.9 to 2.7 per mil (Hwacheon, 2.7‰; Daeweon, −1.7 and 0.9‰; Kuryong, −2.8 and 1.9‰; Cheongryong, −9.9 and −5.6‰) (Table 2).

Inclusion fluids were extracted from nine samples of vein minerals (7 from quartz and 2 from calcite) and their waters were analyzed for hydrogen isotope composition. The ranges of δD values of inclusion waters are: stage I quartz, −65 to −80 per mil (Hwacheon, −65‰; Daeweon, −79 and −80‰; Kuryong, −62 and −71‰; Cheongryong, −72 and −79‰); stage III calcite from Kuryong deposit, −75 and −76 per mil (Table 2).

The $\delta^{18}O$ values of two stage III calcite from the Kuryong deposit are 3.4 and 3.9 per mil (Table 2). Using the calcite-water oxygen isotope fractionation equation of Matsuhisa *et al.* (1979), coupled with temperature estimates based on fluid inclusions and paragenetic constraints, the $\delta^{18}O$ values of waters in equilibrium with the calcites are −5.9 and −6.4 per mil. The $\delta^{13}C$ values for calcites range from −7.1 to −7.5 per mil.

Interpretation of Oxygen and Hydrogen Isotope Results

Fig. 7 shows the distribution of measured and calculated hydrothermal fluid compositions for the Hwacheon-ri mineralized area and the presumed meteoric water at the time of mineralization on conventional diagram of oxygen versus hydrogen isotope compositions.

In order to assess the importance of meteoric water in the hydrothermal system and to interpret the measured δD values of inclusion waters, it is important to know the δD value of the local meteoric water at the time of mineralization. Shelton et al. (1990) recently measured δD values of inclusion waters in vein minerals from Korean hydrothermal vein deposits of Cretaceous age. The total range of these δD value is −44 to −143 per mil. Within the range, the δD value of approximately −80 per mil, based on the δD values (−75 to −79‰)

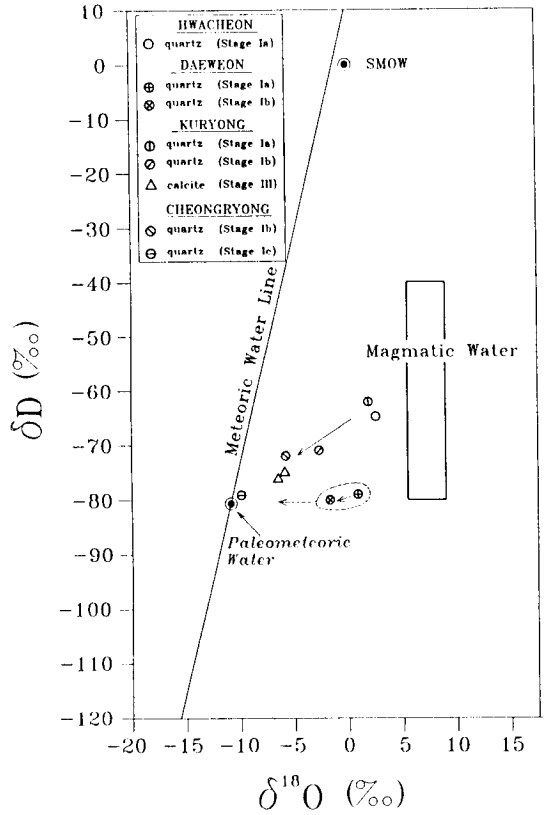

Fig. 7. Hydrogen versus oxygen isotope diagram displaying hydrothermal fluid compositions from each mine in the Hwacheon-ri mineralized area. Meteoric water line is from Craig (1961); magmatic water box is from Taylor (1974).

for inclusion waters from stage Ic quartz and stage III calcites, has been assumed for the unexchanged local meteoric water during the mineralization in the mineralized area. This value is also estimated from the δD value of stage I quartz from the vein of the Daeweon deposit. The quartz has δD values that are lower (−80 and −79‰) than those of the vein minerals from the other deposits in the area and $\delta^{18}O$ values that are intermediate between meteoric and magmatic water (Table 2 and Fig. 7). Field and Fifarek (1985) proposed that such a trend, known as the 'oxygen isotope shift', was characterized by increasing values of $\delta^{18}O$ at nearly constant δD.

The relationship of calculated $\delta^{18}O$ water values in the mineralized area to mineral paragenesis and temperature indicates a systematic decrease from values of 2.3 per mil for substage Ia mineralization, to −2.0 per mil for substage Ib mineral deposition, to −9.9 per mil for substage Ic mineralization (Fig. 7). The δD values of fluid inclusion waters also suggests a systematic decrease with paragenetic time from −62 per mil to −79 per mil, all but two quartz samples (substage Ib) from the Daeweon deposit. This systematic decrease of $\delta^{18}O$ water and δD values with increasing paragenetic time indicates a progressive increase of meteoric water interaction in the hydrothermal system of the area.

Quartz from the substage Ia (early mineralization of stage I) in the Hwacheon and Kuryong deposits yielded isotopic values which fall outside the calculated range of magmatic water (Taylor, 1974) toward negative $\delta^{18}O$ value. This may therefore represent that the initial hydrothermal fluids at Hwacheon-ri were derived from a paleometeoric water that became isotopically highly evolved through isotope exchange reaction with igneous rocks (such as Masanite and/or volcanic rocks in the mineralized area) at elevated temperature (≥370℃) under low water/rock ratios. Isotopic values from the substage Ib and Ic quartz and stage III calcite fall significantly outside the range of magmatic and substage Ia water toward more negative oxygen and hydrogen isotope values. These could signify a mixing of highly exchanged meteoric water with unexchanged meteoric water, or exchange of meteoric water with igneous rock at elevated temperatures and high water to rock ratio.

The lowest δD values (−80 and −79‰) and the moderate $\delta^{18}O$ values (−1.7 and 0.9‰) of the waters (dotted circle area shown in Fig. 7) that deposited stage I minerals at the Daeweon deposit may indicate deposition from an isotopically moderately evolved meteoric water that underwent high ^{18}O enrichment but low D enrichment, reflecting moderate ratios of water to rock (about 0.5 to 0.1; Choi *et al.*, 1993, Field and Fifarek, 1985; Taylor, 1974). Although we have insufficient O-H isotope data for the Daeweon deposit, the data may be consistent with meteoric water dominance as fluid compositions approach those of local, unexchanged meteoric waters (dotted arrows in Fig. 7).

In summary, the isotopic compositions of fluid in the Hwacheon-ri hydrothermal system indicate a progressive shift from a dominance of highly exchanged meteoric water in substage Ia towards an unexchanged meteoric water in substage Ic and stage III.

GEOCHEMICAL ENVIRONMENTS OF ORE DEPOSITION

Equilibrium thermodynamics are used to estimate the changes in chemical conditions of the hydrothermal fluids during ore and gangue minerals deposition in the Hwacheon-ri hydrothermal system. Ranges of temperature and fugacity of sulfur (fs_2) were estimated from phase relations and mineral compositions in the systems

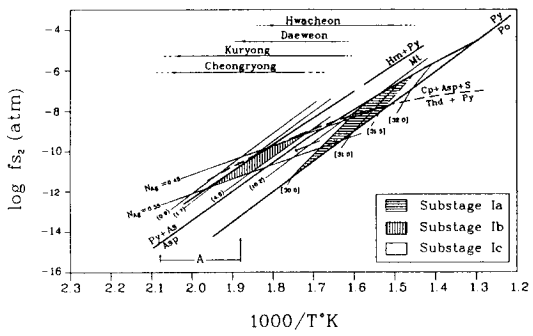

Fig. 8. Fugacity of sulfur versus temperature diagram showing the evolutionary trend of hydrothermal fluids at the Hwacheon-ri mineralized area. "A" represents the range of homogenization temperature of fluid inclusions in substage Ic sphalerite. Abbreviations : As = native arsenic, Asp = arsenopyrite, Cp = chalcopyrite, Hm = hematite, Mt = magnetite, NAg = atomic fraction of Ag in electrum, Po = pyrrhotite, Py = pyrite, S = native sulfur, Thd = tetrahedrite. Numbers in square brackets : As content of arsenopyrite, atomic %; numbers in round brackets : FeS content of sphalerite, mol %.

Fe-As-S (Kretschmar and Scott, 1976), Fe-Zn-S (Scott and Barnes, 1971), Au-Ag-S (Barton and Toulmin, 1964), and Fe-O-S (Helgeson, 1969). These ranges are shown in Fig. 8.

Arsenopyrite is closely associated with pyrite in the early mineralization (occurred dominantly at the Hwacheon deposit) of stage I (substage Ia) and occurs with pyrrhotite and early sphalerite with high FeS contents (down to 10.2 mole %). The As contents of arsenopyrite in substage Ia mineralization range from 30.3 to 31.5 atomic %. These correspond to log fs_2 values and precipitation temperatures from -6.5 to -11.5 and from 300° to 410℃, respectively (Fig. 8). Pyrite ± sphalerite ± electrum ± chalcopyrite ± tetrahedrite assemblages (sphalerite, 1.7~4.6 mole % FeS; electrum, N_{Ag}= 0.45~0.55) in substage Ib were precipitated over a temperature range of ≈ 245° to 325℃, which corresponds to fs_2 values of 10~11.8 to 10~9.0 atm. The latest mineralization of stage I vein contains more iron-poor sphalerite (≤0.9 mole % FeS), hematite, and pyrite. The homogenization temperatures of late substage Ic sphalerite coupled with the homogenization temperatures of fluid inclusions associated stage I quartz suggest that the formation temperatures of substage IIc were 205° to 260℃. Based on these formation temperatures, the range of fs_2 values is 10~10.2 to 10~12.5 atm.

It is further possible to define chemical changes responsible for mineral deposition by using a fugacity of sulfur (fs_2) versus fugacity of oxygen (fo_2) diagram (Figs. 9 and 10). The diagrams, for convenience, have been constructed for temperatures of 300°, and 250℃ in order to facilitate comparison of the chemical changes in the substage Ia-Ib, and Ib-Ic, respecitvely. Additionally, diagram for fo_2-fs_2 (presented by dotted reaction line in Fig. 9) is constructed assuming ore fluid temperatures of 350℃ for the early mineralization (substage Ia) of stage I. The occurrence of pyrite + pyrrhotite + arsenopyrite (+sphalerite) assemblage and absence of magnetite and graphite in the early mineralization (substage Ia) of stage I allow reconstruction of the minimum and maxmimum values of log fo_2 of -32.4 and -29.3, respectively. For the late substage Ia mineralization at and/or near 300℃, which is characterized by pyrite + pyrrhotite + magnetite assemblage, the mean fo_2 value is defined by the FeS_2-FeS-Fe_3O_4 reaction ($fo_2 \approx 10^{-33.9}$ atm, Fig. 9). The occurrence of pyrite and absence of magnetite and graphite in the substage Ib allow reconstruction of maximum and minimum values of log $fo_2 \approx -31.3$ and -35.0, respectively. The absence of magnetite in the late of substage Ib mineralization coupled with sphalerite compositions (1.7~4.6 mole % FeS) indicates that the maximum value of log fo_2 was < -34.6. The minimum value of log fo_2 during the late mineralization of substage Ib may be estimated from the occurrence of rhodochrosite and absence of alabandite. Assuming a log f_{CO_2} value of 0.6 atm (based on the fluid inclusion data and Henry's law constant; Ellis and Golding, 1963), the minimum log fo_2 value for the late mineralization of substage Ib is approximately -38.3 (Fig. 10). The characteristic occurrence of hematite in the substage Ic mineralization can be used to define the fo_2 condition by combining with the mean value of FeS content (≈ 0.9 mole % FeS) in the latest sphalerite which occurs near and in vugs. Obtained value of log fo_2 at 250℃ of substage Ic mineralization is ≥ -33.8 (Fig. 10). This value may be a minimum value of fo_2 in substage Ic ore fluid, for chalcocite and hematite assemblage occurrence in substage Ic.

In summary, ranges of both variables (temperature and fs_2) for the ore fluids of each substage in the stage I mineralization decreased with paragenetic time. The decrease in $\delta^{34}S$ values of H_2S during substage Ic mineralization (toward 1.6‰) reflects more oxidizing conditions during the final collapse of the meteoric hydrothermal system which eventually resulted in carbonate deposition. The presence of the assemblage hematite + sulfides in the later mineralization of the stage I (Fig. 3), as well as the variations of sphalerite compositions, attests to relatively oxidizing fluid conditions. The progressive decreases in temperature and fs_2 and apparent concomitant increase in fo_2 coupled with above men-

Solubility data given by Helgeson (1969), Crerar and Barnes (1976), and Seward (1984) combined with the geochemical variables (fs_2, pH, fo_2 and $\sum S$ at each temperature relating Cu mineralization) from the Hwacheon-ri hydrothermal system suggest that the chloride complexes were effective transporting ligands of Cu in the ore fluids. Copper becomes progressively more soluble with increasing oxygen activity as chloride complexes (Crerar and Barnes, 1976) even in dilute chloride solutions (Fig. 11). Thus copper becomes relatively increasingly important in mineralized veins as uplift progresses and unexchanged meteoric water comes to dominate over initial highly exchanged meteoric water (exchange with igneous rocks at elevated temperature and low water/rock ratios) (see section on Interpretation of Oxygen and Hydrogen Isotope Results). Figs. 9 and 10 show the increasing tendencies of fo_2 at temperature range ($\approx$ 300° to 240℃) with progressive dominance of unexchanged meteoric water. The presence of the assemblage hematite + sulfides in the later mineralization of the stage I (Fig. 3), as well as the sphalerite compositions, attests to relatively oxidizing fluid conditions at the temperature range. The increasing oxidizing nature of the later stage I (later mineralization period of substage Ib to substage Ic) fluids may have led to decrease amounts of chalcopyrite precipitation. Futhermore, copper is highly soluble in more oxidized fluids and more extensive mobilization from the country rocks might be expected at later period mineralization when meteoric incursion occurs. Precipitation and concentration of these copper from the fluid of the later stage I occur in or near vugs in stage I quartz. These may be due to rapid cooling at the latest ore mineralization.

In summary, copper mineralization in the Hwacheon-ri hydrothermal system occurred as follows. 1) Oxidized meteoric fluids moved through the highly fractured near-surface rocks, warm progressively and could dissolve more copper (main chloride complexes) by exchange of meteoric water with igneous rocks (volcanic rocks and Masanite as host rocks) (see section on Interpretation of Oxygen and Hydrogen Isotope results). 2) This initial highly exchanged meteoric water convected in Hwacheon-ri hydrothermal system. 3) Copper solubility in the heated (> 300℃) fluid then decreased with low water to rock ratio due to decreasing oxygen activity (Figs. 9 and 11). Hence copper mainly precipitated at early mineralization (from the substage Ia to early period of substage Ib) of the stage I. 4) Unexchanged meteoric water came over initial highly exchanged meteoric water at later period of the substage Ib (see section on Fluid Inclusion Studies) and then copper precipitation were decreased by increasing oxygen activity. 5) Residual and added copper (copper mobilization into the hydrothermal system from the country rocks by progressive oxidized meteoric water incursion) were precipitated and concentrated in or near vugs in quartz as the latest ore mineralization of stage I vein by rapid cooling (more pronounced mixing of unexchanged meteoric water).

ACKNOWLEDGEMENTS

This paper was supported by NON DIRECTED RESEARCH FUND, Korea Research Foundation. The authors acknowledge also the Center for Mineral Resources Research for partial support for field survey and stable isotope analyses.

REFERENCES

Barton, P.B., Jr. and Toulmin, P. III (1964) The eletrum tarnish method for determination of the fugacity of sulfur in laboratory sulfide systems. Geochim. et Cosmochim. Acta, v. 33, p. 841-857.

Choi, S.H. and So, C.S. (1992) Mineralogy and geochemistry of the Keumhak Cu vein deposit, Korea. Jour. Min. Pet. Econ. Geol., v.87, p. 69-85.

Choi, S.H., So, C.S., and Lee, J.H. (1993) Mineralogical, stable isotope and fluid inclusion studies of copper-bearing hydrothermal vein deposits in Goseong mining district, Gyeongsang basin, Korea. Trans. Inst. of Mining and Metallurgy, v. 102, p. B123-B133.

Choi, S.H., So, C.S., Kweon, S.H., and Choi, K.J. (1994) The geochemistry of copper-bearing hydrothermal vein deposits in Goseong mining district (Samsan area), Gyeongsang basin, Korea. Econ. Environ. Geol., v. 27, p. 147-160.

Craig H. (1961) Isotopic variations in meteoric waters. Sciences, v. 133, p. 1702-1703.

Crerar D.A. and Barnes H.L. (1976) Ore solution chemistry: V. Solubilities of chalcopyrite and chalcocite assemblages in hydrothermal solution at 200 to 350℃. Econ. Geol., v. 71, p. 772-794.

Cunningham, C.G. (1978) Pressure gradients and boiling as mechanisms for localizing ore in porphyry systems. U.S. Geol. Survey J. Research, v. 6, p. 745-754.

Ellis, A.J. and Golding, R.M. (1963) The solubility of carbon dioxide above 100℃ in water and sodium chloride solutions. Am. Jour. Sci., v. 261, p. 47-60.

Field, C.W. and Fifarek, R.H. (1985) Light stable isotope systematics in the epithermal environment. in Geology and Geachemistry of Epithermal Systems. Reviews in Econ. Geol., v. 2, p. 99-128.

Grinenko, V.A. (1962) Preparation of sulfur dioxide for isotopic analysis. Neorganisch, Khimii, v.7, p. 2478-2483.

Hall, W.E. and Friedman, I. (1963) Compositions of fluid inclusions, Cave-in-Rock fluorite district, Illinois, and Upper Mississippi Valley lead-zinc district. Econ. Geol., v.58, p. 886-911.

Helgeson, H.C. (1969) Thermodynamics of hydrothermal

systems at elevated temperatures and pressures. Am. Jour. Sci., v. 267, p. 729-804.

Hass, J.L., Jr. (1971) The effect of salinity on the maximum thermal gradient of a hydrothermal system at hydrostatic pressure. Econ. Geol., v. 66, p. 940-946.

Hedenquist, J.W. and Henley, R.W. (1985) The importance of CO_2 on freezing point measurements of fluid inclusions: Evidence from active geothermal systems and implications for epithermal ore deposition. Econ. Geol., v. 80, p. 1379-1406.

Iiyama, J.T. and Fonteilles, M. (1981) Mesozoic granitic rocks of southern Korea reviewed from major consituents and petrography. Mining Geology, v. 31, p. 281-296.

Ishihara, S., Lee, D.S., and Kim, S.Y. (1981) Comparative study of Mesozoic granitoids and related W-Mo mineralization in southern Korea and southwestern Japan. Mining Geology, v. 31, p. 311-320.

Jin, M.S., Kim, S.Y., and Lee, J.S. (1981) Granitic magmatism and associated mineralization in the Gyeongsang basin, Korea. Mining Geology, v. 31, p. 245-259.

Kim, J.H. and Kim, J.T. (1963) Geological Map of Korea: Masan Sheet, Sheet-6919-IV, Geological Survey of Korea, 26p.

Kretschmar, U. and Scott, S.D. (1976) Phase relations involving arsenopyrite in the system Fe-As-S and their application. Canadian Mineralogist, v. 14, p. 364-386.

Lee, D.S. (1987) Geology of Korea, Kyohak-Sa, Seoul, 514p.

Matsuhisa, Y., Goldsmith, R., and Clayton, R.N. (1979) Oxygen isotope fractionation in the system quartz-albite-anorthite-water. Geochim. Cosmochim. Acta, v. 43, p. 1131-1140.

McCrea, J.M. (1950) The isotopic chemistry of carbonates and a paleotemperature scale. J. Chem. Physics, v. 18, p. 849-857.

Ohmoto, H. and Rye, R.O. (1979) Isotopes of sulfur and carbon in Barnes, H.L., ed., Geochemistry of hydrothermal ore deposits. New York, Wiley Intersci., p. 509-567.

Park, H.I., Choi, S.W., Chang, H.W., and Lee, M.S. (1983) Genesis of the copper deposits in Goseong district, Gyeongnam area. Jour. Korean Inst. Mining Geol., v. 16, p. 135-147.

Park, H.I., Choi, S.W., Chang, H.W., and Chae, D.H. (1985) Copper mineralization at Haman-Gunbuk mining district. Jour. Korean Inst. Mining Geol., v. 18, p. 107-124.

Potter, R.W., III and Clynne, M.A. (1978) Solubility of high soluble salts in aqueous media-part 1, NaCl, KCl, $CaCl_2$, Na_2SO_4, and K_2SO_4 solubilities to 100℃. U.S. Geol. Survey Jour. Research, v. 6, p. 701-705.

Roedder, E., Ingram, B., and Hall, W.E. (1963) Studies of fluid inclusions III. Extraction and quantitative analysis of inclusion in the milligram rane. Econ. Geol., v. 58, p. 363-374.

Rye, R.O. (1966) The carbon, hydrogen, and oxygen isotope composition of the hydrothermal fluids responsible for the lead-zinc deposits at Providencia, Zacatecas, Mexico. Econ. Geol., v. 61, p. 1399-1427.

Scott, S.D. and Barnes, H.L., 1971, Sphalerite geothermometry and geobarometry. Econ. Geol., v. 66, p. 653-669.

Shelton, K.L., So, C.S., Haeussler, G.T., Chi, S.J., and Lee, K.Y. (1990) Geochemical studies of the Tongyoung Gold-Silver Deposits, Republic of Korea: Evidence of Meteoric Water Dominance in a Te-Bearing Epithermal System. Econ. Geol., v. 85, p. 1114-1132.

Sillitoe, R.H. (1980) Evidence for porphyry-type mineralization in Southern Korea. Mining Geol. Special Issue, v. 8, p. 205-214.

So, C.S., Chi, S.J., and Shelton, K.L. (1985) Cu-bearing hydrothermal vein deposits in the Gyeongsang Basin, Republic of Korea. Econ. Geol., v. 80, p. 43-56.

Taylor, H.P., Jr. (1974) The application of oxygen and hydrogen isotope studies to problems of hydrothermal alteration and ore deposition. Econ. Geol., v. 69, p. 843-883.

Manuscript received 26 July 1995

경상분지내 열수동광상의 지화학 및 성인연구 : 화천리지역 광화대

소칠섭 · 최상훈 · 윤성택

요 약 : 경상분지 백악기 화산암류내 배태된 함동열수맥상광체들로 구성된 화천리지역 동광상(대원, 구룡, 청룡, 화천)들은 구조운동에 수반되어 3회(I, II, III)에 걸쳐 광화작용이 진행되었다. 주 광화시기인 광화 I기는 광물들의 산출조직과 공생관계 등에 의하여 3개의 substage (Ia, Ib, Ic)로 구분되며, 황철석, 유비철석, 자류철석, 자철석, 황동색, 에렉트럼, 섬아연석, 방연석, 적철석 등의 광석광물들이 주로 산출된다. 이들 광물조성은 지역내 각 광상에서 유사하지만, 몰리브덴의 산출이 관찰되는 화천광상의 경우 광화I기 초기(Ia)의 광화작용이, 구룡과 청룡광산에서는 적철석의 산출로 특징지어지는 광화I기 후기(Ic)의 광화작용이 각각 우세하게 진행되었다. 이러한 결과는 관계화성암과 관련된 지역내 각 광상의 공간적 분포상태에 따른 열수유체의 진화정도에 의해 지배되었을 것으로 사료된다. 유체포유물 연구결과, 광석광물의 주된 침전은 9~1 wt. % 상당염농도를 갖는 광화유체로부터 350°에서 200℃에 걸쳐 진행되었다. 광화유체내 산소, 수소, 안정동위원소 연구결과, 화천리지역 열수계의 광화유체내 산소 안정동위원소비값이 광화작용의 진행에따라 2.7‰로 부터 후기 −9.9‰로 감소함은 수소 안정동위원소비값의 감소 (−62‰→−80‰)와 함께, 상대적으로 낮은 water/rock 비값을 갖는 환경하에서 동위원소 교환반응을 이뤄 평형상태에 이른 초기 열수계내에 차갑고 동위원소적 교환반응이 거의 이뤄지지않은 천수의 혼입이 점증하였음을 보여준다. 이러한 광화유체의 진화양상과 광상내 산출하는 광물공생관계 및 화학조성에 의한 열역학적 고찰결과는, 광화유체내 Cu는 주로 chloride complex상으로 이동되었으며, 이의 침전은 주로 천수유입에 의한 fo_2의 변화와 온도감소에 의하여 지배되었음을 알 수 있다.